Resonant characteristics of statistical fluctuations in $^{12}C + {}^{12}C$ reaction cross sections

D. L. Gay
Department of Natural Sciences, University of North Florida, Jacksonville, Florida 32216

L. C. Dennis
Department of Physics, Florida State University, Tallahassee, Florida 32306

(Received 24 August 1992)

The effects of angular momentum conservation on the properties of Ericson fluctuations in cross sections for the $^{12}C(^{12}C,{}^{8}Be_0)^{16}O$(g.s.) reaction and $^{12}C(^{12}C,\alpha)^{20}Ne^*$ reactions leading to the 12 lowest excitations in ^{20}Ne are studied. Comparison of Hauser-Feshbach predictions to experimental measurements of the $^{8}Be_0$ total cross section in the range $9 \leq E_{c.m.} \leq 20$ MeV indicates that this reaction channel is populated primarily by a compound-nucleus mechanism. Similar results are obtained for the majority of the α-particle channels in the energy region from $E_{c.m.} = 6.5$ to 12.6 MeV. The compound-nucleus cross sections for these reactions are dominated by a narrow range of angular momenta. A statistical model that includes predicted unequal contributions from compound-nucleus levels with different spins is used to synthesize angular distributions and excitation functions for comparison to data. The results of these simulations give overall quantitatively correct estimates of the size and frequency of the fluctuations observed in the measured total cross sections and of the spins that dominate the fluctuations. Consequences for the identification of "resonances" are discussed.

PACS number(s): 24.60.Dr, 24.60.Ky, 25.70.Ef

I. INTRODUCTION

The nature of the energy-dependent fluctuations in $^{12}C+{}^{12}C$ reaction cross sections is one of the long outstanding problems in heavy-ion physics. Continued interest in $^{12}C+{}^{12}C$ induced reactions has been motivated largely by the discovery [1] at energies near and below the Coulomb barrier of several "resonance" structures characterized by widths < 200 keV. These structures have the unique feature of appearing in all of the examined exit channels at the same energies and are generally considered to originate from a nonstatistical reaction mechanism. Structures observed at energies above the barrier region do not exhibit the same degree of cross-channel correlation and are characterized by widths ranging from < 100 to ≈ 500 keV, which are similar to the widths predicted by statistical models for Ericson fluctuations [2]. Various researchers have used a variety of methods to distinguish nonstatistical structures from fluctuations. Criteria used to locate "resonances" in data typically include requirements similar to the following: (1) The structure should appear in angle-integrated, or total, cross sections [3–7]. (2) For spin-zero exit channels, angular distributions measured near maxima should exhibit shapes characteristic of a single dominant angular momentum value [3–8]. (3) The structure should persist when excitation functions measured for many different exit channels are summed [5, 6, 9]. (4) Structure should appear correlated in several exit channels [3, 8, 9]. The energies and J^π values of reported $^{12}C+{}^{12}C$ "resonances" are summarized elsewhere [7, 10]. Curiously, some of the "resonances" have been reported in reaction channels and within energy regions where fluctuation analyses have been performed [11, 12] with results that support a statistical origin for the same structures. The present work begins the process of resolving these contradictory results by using computer-generated excitation functions and angular distributions to examine the properties of Ericson fluctuations in several $^{12}C+{}^{12}C$ reaction channels in order to determine whether the fluctuations exhibit characteristics that the criteria listed above attribute to "resonances."

Statistical fluctuations originate in the random interference of the overlapping compound-nucleus levels excited by the reaction [2, 13]. The degree to which the levels overlap is expressed quantitatively by the ratio Γ/D, where Γ is the average coherence width and D is the average spacing of the excited levels. Other authors [14–16] have discussed the effect of varying the degree of overlap on the average properties of fluctuations. In Ref. [14] a study of computer-synthesized excitation functions shows that statistical approximations are valid for conditions where $\Gamma/D \gtrsim 2$. The strong dependence of the nuclear level density on spin ensures that the degree of overlap achieved by a reaction changes rapidly with angular momentum. Sufficient overlap must be obtained for each spin, i.e., $\Gamma^J/D^J \gtrsim 2$ for each J value, for fluctuations to be considered statistical.

A computer model for calculating synthetic excitation functions and angular distributions which includes conservation of angular momentum has been presented in a prior publication [17]. This model simulates the detailed behavior of the cross sections by summing over a large number of Breit-Wigner resonances for which the energies and amplitudes are selected randomly. Other studies

of statistical fluctuations have been carried out using such synthetic "data" [12, 14, 15]. The key difference here is that this computer model accounts for the unequal distribution of the entrance channel flux to compound-nucleus states with different spins and the variation in the number of decay channels open to each angular momentum. These features are incorporated into the model by requiring that the energy-averaged value of an individual fluctuating partial cross section approximately equal the Hauser-Feshbach cross section [18] for that spin. The average spin and energy dependences of all the resonance parameters, e.g., the coherence widths, level spacings, numbers of open decay channels, etc., used in the simulations are determined from existing experimental data. In another publication [19], synthetic excitation functions and angular distributions generated by this model are compared to experimental cross sections for the reaction ^{16}O(^{16}O,α_0)^{28}Si. The synthetic fluctuations reproduce the size and frequency of the structures in the data as well as the spins that dominate the measured angular distributions.

This paper extends the study of the characteristics of Ericson fluctuations in reaction cross sections to the ^{12}C+^{12}C system and, in the process, shows explicitly for the first time how the simulation of angular distributions and excitation functions provides information on the nature of compound-nucleus reactions that complements the information obtained from Hauser-Feshbach calculations. The quantitative simulation of fluctuations is described for ^{12}C+^{12}C reactions leading to the ^{8}Be$_0$(g.s.) exit channel and the α-particle exit channels leading to the 12 lowest excitations in ^{20}Ne. These exit channels were chosen for study because published cross sections for the ^{8}Be$_0$ channel [4, 7] and the α-particle channels [6] have been measured at sufficiently small energy intervals and over energy and angular ranges sufficiently broad to permit a more meaningful comparison between the data and the simulations. Several of these reactions have an exit channel spin of zero, which facilitates the study of the angular momenta that dominate the experimental and synthetic cross sections. Finally, the authors who published these two sets of data have employed different combinations of the criteria listed above to isolate "resonances" in their data. The goal of this study is to gain further insight into the influence of conservation of angular momentum on the properties of Ericson fluctuations in ^{12}C+^{12}C reaction channels and the extent to which it limits the techniques available for distinguishing nonstatistical structure from fluctuations.

II. CALCULATION OF SYNTHETIC REACTION CROSS SECTIONS

The synthesis of cross sections which result from the statistical decay of overlapping levels of the compound nucleus formed in a reaction necessarily includes many assumptions and simplifications. The method used here to compute fluctuating cross sections for comparison to measured angular distributions and excitation functions is described in this section.

The fluctuation calculations are performed within the framework of the formalism of Blatt and Biedenharn [20], where the differential cross section for a reaction proceeding from an initial state α to a different final state α' is expressed as

$$\frac{d\sigma_{\alpha\alpha'}}{d\Omega}(\theta) = \frac{1}{k_\alpha^2}\frac{1}{(2I+1)(2i+1)} \times \sum_{ss'}\sum_{L=0}^{\infty} B_L(\alpha s;\alpha' s')P_L(\cos\theta), \quad (1a)$$

with Legendre coefficients given by

$$B_L(\alpha s;\alpha' s') = \frac{(-1)^{s-s'}}{4}\sum_{J_1 J_2}\sum_{\ell_1\ell_2\ell_1'\ell_2'} Z(\ell_1 J_1 \ell_2 J_2, sL)Z(\ell_1' J_1 \ell_2' J_2, s'L)\mathrm{Re}\left[S_{cc'}^{J_1\pi_1 *} S_{cc'}^{J_2\pi_2}\right]. \quad (1b)$$

In the above equations, as in all following expressions, unprimed quantities refer to the entrance channel and primed quantities refer to the exit channel. The index α specifies the projectile and target nuclei and their excitations. The channel spin s is formed by vector addition of the respective intrinsic spins I and i of the projectile and target; the channel spin is coupled to the orbital angular momentum ℓ to form the total angular momentum J. Total angular momentum and parity are preserved in compound-nucleus reactions so that J and π are equal to the spin and parity of the compound nucleus. Since different angular momenta can interfere, subscripts are used on the orbital angular momenta in the entrance and exit channels, ℓ and ℓ', respectively, as well as on the total angular momentum. The wave number for the relative motion of the pair of interacting nuclei is k_α. The Z coefficients are standard combinations of Racah and Clebsch-Gordan coefficients [21]. The $P_L(\cos\theta)$ are Legendre polynomials, where θ is the center-of-mass scattering angle and Re[ ] stands for the real part of the quantity within the brackets.

Information on the nature of the reaction mechanism is incorporated into Eq. (1b) via the probability amplitude, or collision matrix element, $S_{cc'}^{J\pi}(E)$, for a collision with total angular momentum J and parity π from an entrance channel state indicated by $c = \alpha s\ell$ to an exit channel state $c' = \alpha' s'\ell'$. For convenience of notation, the parity index π is dropped in succeeding expressions since, for the reactions studied in the present work, all compound-nucleus states formed in single-step processes are of natural parity and π is defined by ℓ and J. Interference arising from the population and decay of overlapping compound-nucleus levels is included explicitly in the differential cross section by assuming that the collision matrix element can be written as a sum of Breit-Wigner terms:

$$S^J_{cc'}(E) = \exp\left[i\left(\Omega^J_c + \Omega^J_{c'}\right)\right] \sum_\mu \frac{i g^J_{c\mu} g^J_{c'\mu}}{E^J_\mu - E - i\Gamma/2}, \qquad (2)$$

where μ is the compound-nucleus level index, E^J_μ and Γ^J_μ are, respectively, the energy and total decay width of the level μ, E is the compound-nucleus excitation energy of the reaction, and Ω^J_c is the Coulomb-plus-nuclear phase shift. The level amplitude $g^J_{c\mu}$ denotes either the positive or negative square root of the partial width $\Gamma^J_{c\mu}$ for decay of the level μ into channel c. Inserting the above expression for the collision matrix element into Eq. (1b), the Legendre coefficients can be written in the following form [22]:

$$B_L(\alpha s;\alpha' s') = \frac{(-1)^{s-s'}}{4} \sum_{J_1 J_2} \sum_{\ell_1 \ell_2 \ell'_1 \ell'_2} Z(\ell_1 J_1 \ell_2 J_2, sL) Z(\ell'_1 J_1 \ell'_2 J_2, s' L)$$
$$\times \sum_{\mu\nu} \left\{ \frac{g^{J_1}_{c\mu} g^{J_1}_{c'\mu}}{\left[\left(E^{J_1}_\mu - E\right)^2 + \left(\frac{1}{2}\Gamma^{J_1}_\mu\right)^2\right]} \frac{g^{J_2}_{c\nu} g^{J_2}_{c'\nu}}{\left[\left(E^{J_2}_\nu - E\right)^2 + \left(\frac{1}{2}\Gamma^{J_2}_\nu\right)^2\right]} \right\}$$
$$\times \{\cos(\Omega^{J_1}_c + \Omega^{J_1}_{c'} - \Omega^{J_2}_c - \Omega^{J_2}_{c'}) \left[\left(E^{J_1}_\mu - E\right)\left(E^{J_2}_\nu - E\right) + \tfrac{1}{4}\Gamma^{J_1}_\mu \Gamma^{J_2}_\nu\right]$$
$$+ \tfrac{1}{2}\sin(\Omega^{J_1}_{c'} + \Omega^{J_1}_c - \Omega^{J_2}_{c'} - \Omega^{J_2}_c) \left[\left(E^{J_1}_\mu - E\right)\Gamma^{J_2}_\nu - \left(E^{J_2}_\nu - E\right)\Gamma^{J_1}_\mu\right]\}. \qquad (3)$$

The total cross section for a reaction from an initial state α to a final state α' can be calculated by integrating over all angles the differential cross section as given by Eq. (1a) [20]:

$$\sigma_{\alpha\alpha'} = \frac{\pi}{k^2_\alpha} \sum_J \frac{2J+1}{(2I+1)(2i+1)} \sum_{ss'\ell\ell'} \left|S^J_{cc'}\right|^2. \qquad (4)$$

Substitution of the the form of the collision matrix element expressed in Eq. (2) into Eq. (4) leads to the desired result for the total fluctuating cross section,

$$\sigma_{\alpha\alpha'} = \frac{\pi}{k^2_\alpha} \sum_J \frac{2J+1}{(2I+1)(2i+1)} \sum_{ss'\ell\ell'} \sum_{\mu\nu} \left\{ \frac{g^J_{c\mu} g^J_{c'\mu}}{\left[\left(E^J_\mu - E\right)^2 + \left(\frac{1}{2}\Gamma^J_\mu\right)^2\right]} \frac{g^J_{c\nu} g^J_{c'\nu}}{\left[\left(E^J_\nu - E\right)^2 + \left(\frac{1}{2}\Gamma^J_\nu\right)^2\right]} \right\}$$
$$\times \left[\left(E^J_\mu - E\right)\left(E^J_\nu - E\right) + \tfrac{1}{4}\Gamma^J_\mu \Gamma^J_\nu\right]. \qquad (5)$$

Equation (5) shows that angular integration removes the interference between amplitudes for compound states with different spins so that the individual partial cross sections σ_J fluctuate independently.

The process of simulating the detailed behavior of a cross section for a particular reaction involves the evaluation of Eqs. (3) and (5) at a number of excitation energies spanning a range broad enough to encompass many fluctuations and at intervals smaller than the average width of the fluctuations. The computer model used in the present work incorporates assumptions and simplifications similar to those initially proposed by Ericson [2, 13] to obtain values for the $g^J_{c\mu}$, E_μ, and Γ^J_μ used to calculate a cross section at each energy. In this model, the overlap of the populated levels in the compound nucleus is assumed to be sufficient for statistical approximations to be applied. Accordingly, the level amplitudes are real random numbers which have a Gaussian distribution with a mean value of zero; level amplitudes in the entrance channel are uncorrelated with those in the exit channel; the dispersion of the level decay widths is neglected, and the widths are assumed to be spin independent, that is, $\Gamma^J_\mu = \Gamma$. Compound-nucleus levels within an energy range $E \pm 4.5\Gamma$ are included in the sums in Eqs. (3) and (5). The energies of the contributing levels are found by using a Fermi-gas-model level-density formula [23] to obtain the average spacing D^J for states of spin J. Each level is then randomly placed within $\pm D^J/2$ of the energy predicted by the Fermi-gas model.

Although the assumptions included in this model reflect a lack of knowledge about the details of the individual overlapping compound-nucleus levels, many are based on physical considerations. The assumption that the dispersion of decay widths is small is appropriate where many decay channels are open [13, 24]. The angular momentum dependence of the decay widths has been found to be weak in many cases [25]. In particular, statistical-model calculations have been used to estimate the dependence on J of average decay widths in ^{24}Mg and have found it to be unpronounced [12]. Average decay widths can be deduced from measured excitation functions by applying the autocorrelation method of Ericson[13] or the peak counting method of Brink and Stephen [26]. A semiempirical evaluation of experimentally deduced average decay widths for various nuclei indicates that the width increases with excitation energy

[12, 27]:

$$\Gamma(\text{MeV}) \approx 14 \exp\left(-4.69\sqrt{A/E}\right), \tag{6}$$

where A is the atomic mass number of the compound nucleus and the excitation energy E is expressed in MeV. Values of Γ used in the present calculations are determined from this relation.

The average size of the fluctuations is fixed by requiring that the energy average of the fluctuating cross section approximate the Hauser-Feshbach cross section. This requirement is expressed in the relation

$$\left\langle \sum_{\mu} \frac{(g^J_{c\mu})^2 (g^J_{c'\mu})^2}{(E^J_\mu - E)^2 + \frac{1}{4}(\Gamma^J_\mu)^2} \right\rangle = \frac{T^J_c(E) T^J_{c'}(E)}{G^J}, \tag{7}$$

in which $T^J_c(E)$ and $T^J_{c'}(E)$ are optical-model transmission coefficients, G^J is the Hauser-Feshbach denominator which is discussed in Sec. III, and the angular brackets denote averaging over compound-nucleus levels. At each energy, transmission coefficients are determined from the relation

$$T^J_c(E) = 1 - \left|\exp(2i\delta^J_c)\right|^2. \tag{8}$$

The complex phase δ^J_c is calculated externally, using an optical-model potential appropriate to the channel, and supplied as input to the computer code. The real part of δ^J_c is substituted for Ω^J_c during the evaluation of Eq. (3).

Equation (7) is used to deduce the variances, $\langle (g^J_{c\mu})^2 \rangle$ and $\langle (g^J_{c'\mu})^2 \rangle$ of the respective Gaussian distributions from which amplitudes in the entrance and exit channels are picked randomly and assigned to each of the levels included in the sums in Eqs. (3) and (5). Values of the $g^J_{c\mu}$ are derived from a sequence of numbers produced by a random-number-generating algorithm [28]. Values of the $g^J_{c'\mu}$ are similarly determined from an independently generated sequence of numbers, so that correlations between fluctuations in different exit channels can be studied for a particular interaction. For this purpose, a separate simulation is performed for each decay channel, wherein the $g^J_{c'\mu}$ for the contributing compound-nucleus levels are selected from a distribution with a variance appropriate to the particular exit channel. The population of the compound-nucleus levels from the entrance channel is modeled by generating a single set of entrance channel amplitudes $g^J_{c\mu}$ which are utilized in all of the separate simulations.

III. HAUSER-FESHBACH CALCULATIONS

The computer model described above synthesizes fluctuating cross sections resulting from compound-nucleus reactions. It is reasonable to expect the frequency and size of the fluctuations generated by this model to be comparable to those observed in experimental cross sections only in those channels where the reactions proceed primarily via a compound-nucleus mechanism. The compound-nucleus contribution to a reaction can be estimated by comparing Hauser-Feshbach (HF) predictions to energy-averaged data.

The Hauser-Feshbach expression for the energy-averaged total cross section is [18, 29–31]

$$\langle \sigma_{\alpha\alpha'} \rangle = \frac{\pi}{k^2_\alpha} \sum_{J\pi} \frac{2J+1}{(2I+1)(2i+1)} \sum_{s\ell} T^J_c \sum_{s'\ell'} \frac{T^J_{c'}}{G^J}. \tag{9}$$

The total width G^J, for the decay of the compound nucleus into all energetically open channels is given by

$$G^J = \sum_{\alpha''\ell''s''} \left[\sum_{E''=0}^{E_c} T_{\alpha''\ell''}(E'') + \sum_{I''\pi''} \int_{E_c}^{E_{\max}} \rho_{\alpha''}(E'', I'', \pi'') \times T_{\alpha''\ell''}(E'') dE'' \right], \tag{10}$$

where the double primes refer to all open channels which couple to angular momentum J. Transmission coefficients for each residual pair are summed over known discrete levels with excitation energies in the range $E'' = 0$ to E_c. Contributions from continuum states at higher energies from E_c to $E_{\max}$, the highest kinematically allowed excitation, are included in the integral over E''. For each parity, the level density for states with spin I'' is calculated from the formula [23]

$$\rho(E'', I'', \pi'') = \tfrac{1}{2} W(E'') F(E'', I''), \tag{11}$$

where the spin dependence is contained in the second factor,

$$F(E'', I'') = e^{-(I'')^2/2\sigma^2} - e^{(I''+1)^2/2\sigma^2}. \tag{12}$$

For low residual excitations, the constant temperature approximation is applied to obtain the first factor in Eq. (11):

$$W(E'') = \frac{1}{T} \exp\left[\frac{E'' - E_0}{T}\right], \qquad E'' < E_x. \tag{13a}$$

At higher excitations, the Fermi-gas expression is applied:

$$W(E'') = \frac{\exp(2\sqrt{aU})}{12\sqrt{2} a^{1/4} U^{5/4} \sigma}, \qquad E'' \geq E_x, \tag{13b}$$

in which U denotes the residual excitation energy E'' minus the pairing energy Δ. The values of the level-density parameters E_0 and T have been determined by fitting the known levels for each residual with Eq. (13a). Values of the level-density parameters a and E_x are then extracted by matching the level densities obtained with Eqs. (13a) and (13b) in slope and magnitude at $E = E_x$ as described in Refs. [23, 32]. The spin cutoff parameter is deduced from the formula given in Ref. [23] with the corrected numerical factor of Ref. [33]:

$$\sigma^2 = 0.1459 \sqrt{aU} A^{2/3}, \tag{14}$$

where A denotes the atomic mass number of the residual, U is in MeV, and A is in MeV^{-1}.

Energy-averaged total cross sections for the ^{12}C(^{12}C,^{8}Be)^{16}O(g.s.) and ^{12}C(^{12}C,α)^{20}Ne* reactions

have been calculated using the computer code HELGA [34]. Since the interacting ^{12}C nuclei are spin-zero particles, ℓ and J are equal in Eq. (9). In addition, because of the identity of the ^{12}C nuclei in the entrance channel, the sums in Eq. (9) are restricted to even values of angular momentum and positive parity, and the resulting cross section is multiplied by a factor of 2. Particle decay channels leading to a total of eight different residual pairs are included in the calculations. Table I shows the parameters used to determine level densities. Parameters for residuals with A < 23 have been determined from known energy levels as described above. The parameters used for proton and neutron channels are derived from a fit, performed by Beckerman [35], of an unusual formulation of the Fermi-gas model to level densities from bound levels and proton resonances in ^{23}Na. Values of a and Δ for ^{23}Mg and ^{23}Na have been extracted by fitting the more conventional form of Eq. (13b) to Beckerman's curve [36].

Transmission coefficients are calculated using potentials, shown in Table II, which have been derived from optical-model evaluations of elastic scattering data for each of the residual pairs except ^{12}C+^{12}C. Since ^{8}Be is unbound to α-particle decay, ^{8}Be+^{16}O elastic scattering data from which optical-model parameters can be extracted do not exist. For the present work, an optical-model parameter set derived from ^{7}Li+^{16}O elastic scattering data [37] has been adopted to calculate ^{8}Be+^{16}O transmission coefficients. The relation of the entrance channel transmission coefficients to the calculated fusion cross section has been employed to choose optical-model parameters for ^{12}C+^{12}C. The fusion cross section is obtained by summing Eq. (9) over all exit channels:

$$\sigma_{\rm fus} = \frac{\pi}{k_\alpha^2}\frac{1}{(2I+1)(2i+1)}\sum_{J,\ell}(2\ell+1)T_c^J. \qquad (15)$$

For those interactions where optical-model potentials derived from elastic scattering data are used, the fusion cross section can be calculated by multiplying each of the T_c^J by a spin- and energy-dependent cutoff factor, which ranges in value from 1 to 0, in order to limit the sum over J. This critical angular momentum cutoff influences the ratio of the HF cross sections for different final states as well as the absolute magnitude of the cross sections [30, 31]. Calculated cross sections are not significantly affected by the form of the critical angular momentum cutoff, whether sharp or smooth, provided that the calculated fusion cross section is equal to the experimentally measured fusion cross section [32]. This condition can be realized without incorporating an explicit critical angular momentum cutoff by using optical-model potentials derived by fitting fusion data to calculate the T_c^J. Hatogai, Ohta, and Okai [38] have used optical-model potentials, which have a short-range imaginary part, to fit measured fusion excitation functions for several light heavy-ion systems. Their parameter set for ^{12}C+^{12}C reproduces the ^{12}C+^{12}C fusion cross sections measured by Kovar *et al.* [39] to within ≈20% at energies from $E_{\rm c.m.} \approx 7.4$ to 20.0 MeV and has been selected for the present calculations.

Hauser-Feshbach predictions are subject to errors due to uncertainties in the parameters used in the calculations. Two sources of uncertainties are considered: level-density parameters and optical-model potentials. Uncertainties in the level-density parameters are primarily statistical errors introduced by the fitting procedures [32] and are approximately 10% for the residuals included in the present calculations. The sensitivity of the calculations to uncertainties in the level-density parameters increases with bombarding energy as more decay channels open to residual levels in the continuum. Reducing the level-density parameters by 10% for all of the residuals produces an increase of less than 10% in the HF cross sections calculated for reactions at center-of-mass energies less than 10 MeV, but generates a 30% increase in the cross sections at $E_{\rm c.m.} = 20$ MeV. The error associated with the optical-model potential used for the entrance channel can be estimated by comparing the fusion cross section calculated with this potential to measured fusion cross sections. As stated above, this error is less than 20%. This straightforward comparison is not available for the residual pairs in the exit channels. The effects of uncertainties in the optical-model potentials for these channels have been estimated by observing the changes in HF cross sections introduced by substituting other appropriate parameter sets for those used in the present work. For example, Frickey, Eberhard, and Davis [40] used several sets of optical-model parameters to fit an-

TABLE I. Level-density parameters used to determine G^J for the Hauser-Feshbach calculations and the fluctuation simulations.

Channel[a]	a (MeV^{-1})	Δ (MeV)	E_0 (MeV)	T (MeV)	E_x (MeV)
^{12}C+^{12}C	1.05	5.00	0.51	6.30	22.73
α+^{20}Ne	2.98	5.13	1.71	2.62	16.38
p+^{23}Na[b]	2.95	1.15			
n+^{23}Mg[b]	2.95	1.15			
^{8}Be+^{16}O	c				
d+^{22}Na	3.21	0.00	−2.64	2.39	9.89
^{3}He+^{21}Ne	3.80	2.50	−0.58	2.14	12.49
^{5}Li+^{19}F	3.20	2.50	−2.31	2.69	16.42

[a]Parameters are for the heavy residual only.
[b]Parameters from Ref. [36].
[c]Discrete levels only.

TABLE II. Optical-model parameters used to calculate transmission coefficients.

Channel	V (MeV)	R_R (fm)	a_R (fm)	W (MeV)	R_I (fm)	a_I (fm)
$^{12}C+^{12}C$[a]	22.70	5.45	0.50	40.00[b]	4.67	0.10
$\alpha+^{20}Ne$[c]	56.90	4.70	0.58	5.18[b]	4.70	0.46
$p+^{23}Na$[d]	$53.67-0.527E_{c.m.}$	3.56	0.65	8.53[e]	3.56	0.47
$n+^{23}Mg$[f]	$47.40-0.310E_{c.m.}$	3.72	0.66	$9.52-0.051E_{c.m.}$ [e]	3.58	0.48
$^{8}Be+^{16}O$[g]	33.10	4.39	0.85	10.30[b]	4.71	0.72
$d+^{22}Na$[h]	$88.85-0.20E_{c.m.}$	3.22	0.81	$14.40+0.22E_{c.m.}$ [e]	3.75	0.68
$^{3}He+^{21}Ne$[i]	$139.00-0.149E_{c.m.}$	3.31	0.72	$44.30-0.289E_{c.m.}$ [b]	3.86	0.86
$^{5}Li+^{19}F$[j]	35.40	4.64	1.05	11.00[e]	5.68	0.62

[a]Parameters from Ref. [38].
[b]Imaginary well is of the volume type.
[c]Parameters from Ref. [40].
[d]F. G. Perey, Phys. Rev. **131**, 745 (1963).
[e]Imaginary well is of the surface type.
[f]D. Wilmore and P. E. Hodgson, Nucl. Phys. **55**, 673 (1964).
[g]Potential for $^{7}Li+^{16}O$ from Ref. [37].
[h]C. M. Perey and F. G. Perey, Phys. Rev. **132**, 755 (1963).
[i]F. D. Bechetti and G. W. Greenlees, as discussed in P. E. Hodgson, *Nuclear Reactions and Nuclear Structure* (Oxford University Press, London, 1971), p. 261.
[j]Potential for $^{7}Li+^{19}F$ from Ref. [37].

gular distributions measured for α-particle scattering by ^{20}Ne. Calculations with these alternate parameter sets generate cross sections for the $\alpha+^{20}Ne$ channels that differ by as much as 70%, while producing changes of less than 10% in the HF denominator and in the cross sections for channels involving other residual pairs. Overall, the calculated cross sections are estimated to be accurate within a factor of 1.5–2.0.

The comparison for the $^{8}Be_0$ exit channel, shown in Fig. 1, of the HF calculation to the data of James and Fletcher [7] indicates that this channel is populated predominantly by compound-nucleus reactions over the entire energy range. The ratio of the data, energy averaged over a running interval of 3 MeV, to the HF cross section ranges from 0.87 to 1.6 and is within the limits of accuracy of the calculations. Comparisons with the cross sections extracted from the publication of Voit *et al.* [6] and shown in Fig. 2 lead to the same conclusion for the majority of the studied α-particle channels. Clear evidence for noncompound processes is found only for the reaction leading to the 7.84-MeV, 2^+ (α_{11}) state in ^{20}Ne, where the HF calculations underpredict the energy-averaged cross section by a factor of at least 2.8 over the range of the data. Earlier studies at higher incident energies have presented evidence that a direct eight-nucleon transfer mechanism is the dominant process in the reactions leading to this state and to other members of a proposed eight-particle–four-hole rotational band based on the 7.20-MeV, 0^+ state [41, 42]. The present comparison indicates that the fraction of the cross section for the 7.84-MeV state that can be attributed to a direct mechanism is not as large as that found at higher energies, but it is at least as significant as that for the compound-nucleus mechanism. The relative importance of direct and compound processes in the cross sections measured by Voit *et al.* for the 7.20-MeV state is not discussed here since their paper does not display a separate excitation function for this channel. Evidence for a direct contribution to the cross section for the first excited 0^+ state at 6.72 MeV (α_6) is not conclusive since the energy-averaged data exceeds the HF cross section by more than the estimated error in the calculation only over the lower two-thirds of the energy range.

A salient characteristic of the compound-nucleus mechanism populating these $^{12}C+^{12}C$ reaction channels is illustrated in Fig. 3, where the histograms of Hauser-

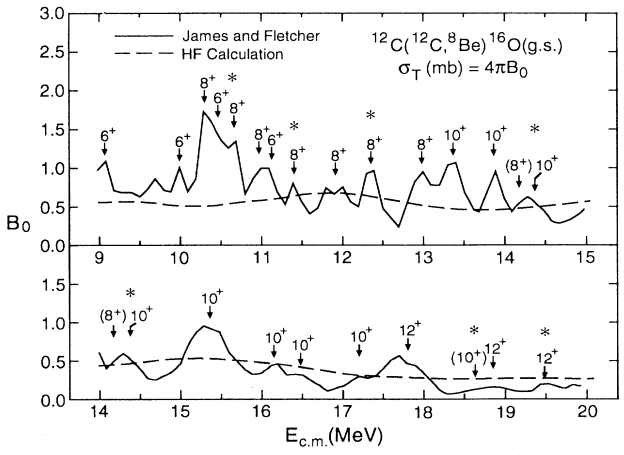

FIG. 1. Comparison of Hauser-Feshbach calculations (dashed line) to the excitation function taken from Ref. [7] for the $^{12}C(^{12}C,^{8}Be_0)^{16}O$ reaction. The authors of Ref. [7] extracted total cross sections by fitting measured angular distributions with a linear expansion of Legendre polynomials. The total cross section is expressed by the zero-order Legendre coefficient B_0. The J^π values and energies of "resonances" reported in Ref. [7] are indicated in the figure. An asterisk indicates a "resonance" observed in other reaction channels.

Feshbach partial cross sections, calculated for $E_{c.m.} = 11$ MeV, show considerable variation with angular momentum. The general shape of these distributions can be explained by taking into account the amount of entrance channel flux available to populate compound states with a particular spin along with the number of open residual channels to which these states can decay. For low spins, many decay channels are open, making small the branching ratio to any one residual state. Larger partial cross sections for higher spins result from the distribution of more entrance channel flux, which varies as $2J + 1$, over fewer open decay channels. The sharp decline near the upper limit of contributing spins starts at a value, slightly less than the grazing angular momentum, where the transmission coefficients decrease rapidly with increasing orbital angular momentum. The grazing angular momentum in either the entrance channel or the exit channel can fix the upper limit, depending largely on the final state spin and Q value. A sufficiently large negative final state Q value produces an exit channel grazing angular momentum smaller than the entrance channel grazing angular momentum. This results in a corresponding reduction of the partial cross sections for higher spins if the exit channel spin is small. The effect of poorly matched entrance and exit channels is evident in the distributions for the first (α_6) and second (α_9) excited 0^+ states in ^{20}Ne where the $J = 8$ partial cross sections are suppressed in comparison to the other well-matched exit channels. Figure 4 shows that the general characteristics of the partial cross sections calculated at $E_{c.m.} = 11$ MeV extend to other energies. At each energy, a narrow range of spins dominate the cross section with higher spins gaining significance as the reaction energy increases.

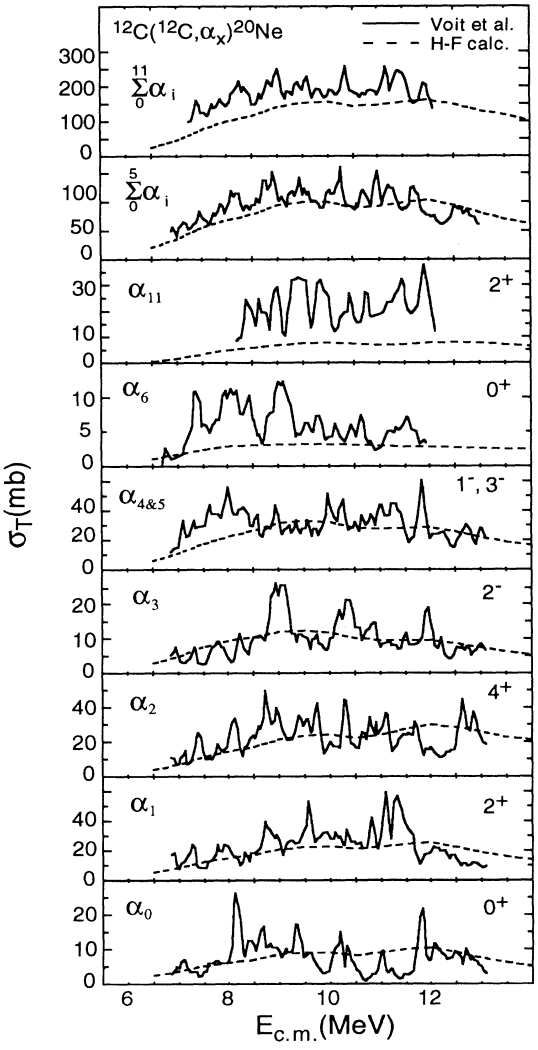

FIG. 2. Comparison of Hauser-Feshbach total cross sections to excitation functions of total cross sections taken from Ref. [6] for ^{12}C(^{12}C,α)^{20}Ne* reactions leading to the seven lowest excitations in ^{20}Ne and to the 7.84-MeV, 2^+ state in ^{20}Ne. The two uppermost panels show the comparisons for cross sections summed over the lowest 6 and lowest 12 excitations in ^{20}Ne.

IV. SYNTHETIC EXCITATION FUNCTIONS AND ANGULAR DISTRIBUTIONS

The HF predictions indicate that the size of the fluctuations in these ^{12}C+^{12}C reaction channels is strongly dependent on the spin of the underlying compound states. The average size of the fluctuations for each spin value is determined by the variances of the level amplitude distributions as given by Eq. (7) in Sec. II. Significant contributions to the fluctuating cross section are restricted to two or three successive even spins near the grazing angular momentum. For the lower spins, the fluctuations about the average cross section are limited in size by the large number of open decay channels. The strong localization of the partial cross sections for these reaction channels provides a physical basis for simplifying the synthesis of excitation functions and angular distributions. Level amplitudes are summed coherently for the three most significant J values at each reaction energy, while the small contributions from compound states with lower spins are approximated by the corresponding Hauser-Feshbach partial cross sections. For the simulations discussed below, the three J values for which compound-nucleus levels have been included explicitly in the evaluation of Eqs. (3) and (5) are $J = 2$, 4, and 6 at center-of-mass energies less than 9.5 MeV; $J = 4$, 6, and 8 from 9.5 to 12.5 MeV; $J = 6$, 8, and 10 from 12.6 to 16.1 MeV; and 8, 10, and 12 at energies above 16.1 MeV. This approximation reduces the computation times and computer memory requirements by as much as two orders of magnitude and makes it feasible to synthesize angular distributions and excitation functions.

The variation of the fluctuating cross section with energy and angle is influenced by the average decay width and density of the compound-nucleus levels insofar as the value of Γ determines the coherence width for the interference of a number of levels which is fixed for each spin by the value of ρ^J. The density of states in ^{24}Mg has been calculated from the Fermi-gas level-density formula given by Eqs. (11), (12), and (13b) using values obtained from

Ref. [43] for the level-density parameter, $a = 2.92$, and the pairing energy, $\Delta = 2.2$. The average decay width at each reaction energy has been determined by evaluating Eq. (6). The synthesized fluctuations incorporate values for Γ that range from a minimum of 87 keV at $E_{\mathrm{c.m.}} = 6.5$ MeV to 271 keV at 20.0 MeV. Values derived in the Hauser-Feshbach calculations for T_c^J, $T_{c'}^J$, and G^J are used to compute the variances of the distributions from which compound-nucleus level amplitudes are picked as described in Sec. II.

Several of the excitation functions that have been synthesized for the $^{12}C(^{12}C,^{8}Be_0)^{16}O$ reaction are shown in Figs. 5(b)–(e). Cross sections have been calculated at energy intervals of 100 keV in order to approximate the spacing of the data points in the excitation function of James and Fletcher [7], which is shown in Fig. 5(a). Each of the synthetic excitation functions in Fig. 5 has been generated with randomly chosen values for the compound-nucleus level energies and amplitudes in both the entrance and exit channels that are unique. The resulting cross sections in the various excitation functions are uncorrelated, though all of the excitation functions have been calculated with the same average level density, decay width, etc. Several excitation functions are presented for the same reaction in order to emphasize that the cross section at a particular energy cannot be predicted by the statistical model, yet the properties of the fluctuations within a limited energy range can be examined. The structure in the synthetic excitation functions is remarkably similar to that in the data. The calculations generally reproduce the magnitude of the cross sections and, approximately, the density of peaks, which decreases with increasing energy. Peak-to-valley ratios for the structure in the synthetic excitation functions are slightly larger on the average than ≈2:1 ratio found in the data. This difference is probably inconsequential since the simulations do not account for the smoothing effects of the energy and angle averaging that are included necessarily in the measured differential cross sections from which the data in Fig. 5(a) are derived. The

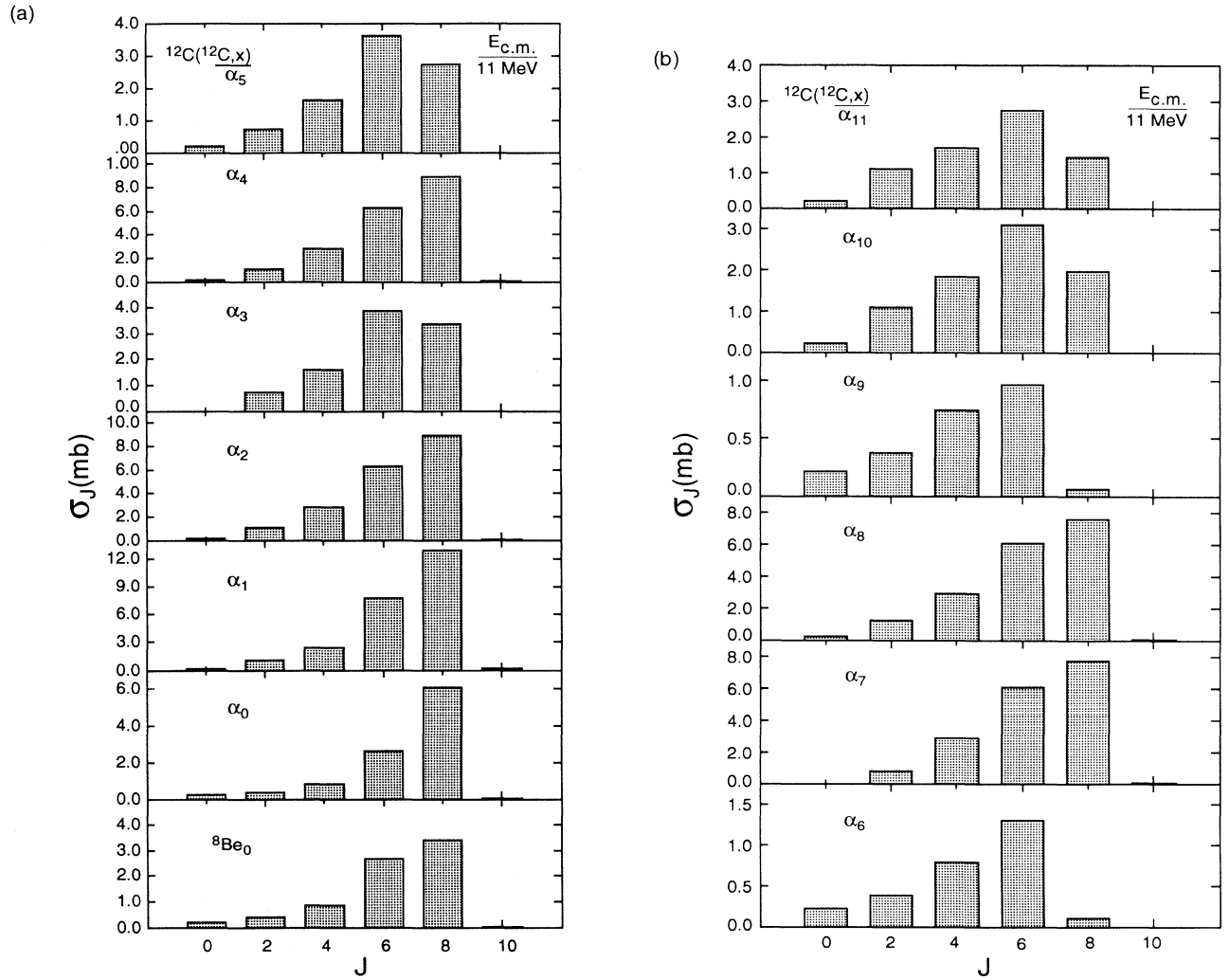

FIG. 3. Angular momentum distributions of Hauser-Feshbach partial cross sections calculated at $E_{\mathrm{c.m.}} = 11$ MeV for the $^{12}C(^{12}C,^{8}Be_0)$ reaction and $^{12}C(^{12}C,\alpha)$ reactions leading to the 12 lowest excitations in ^{20}Ne.

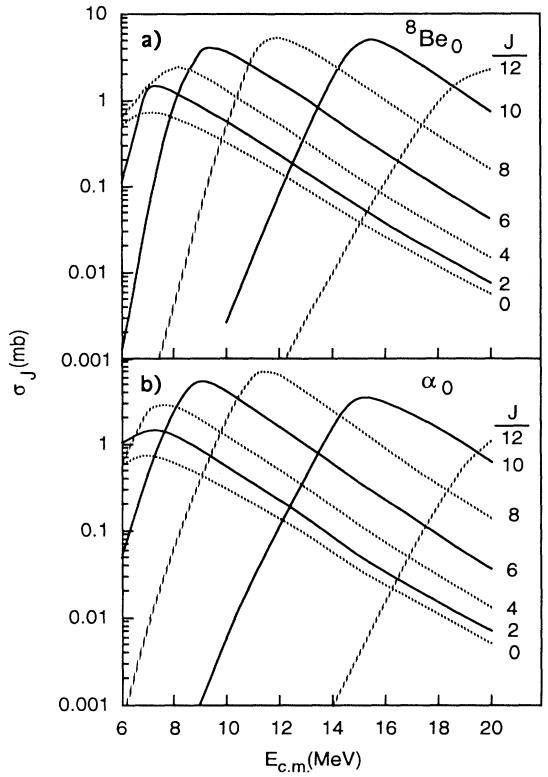

FIG. 4. Hauser-Feshbach partial cross sections versus energy for the reactions $^{12}C(^{12}C,^8Be_0)^{16}O$ and $^{12}C(^{12}C,\alpha_0)^{20}Ne$.

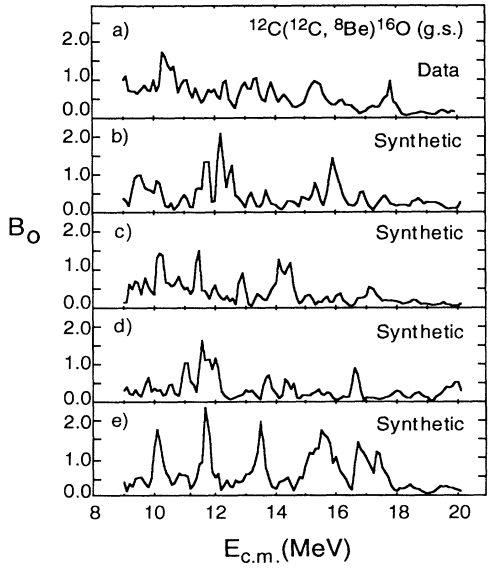

FIG. 5. Several excitation functions synthesized for the $^{12}C(^{12}C,^8Be_0)^{16}O$ reaction are shown in panels (b)-(e) for comparison to the data from Ref. [7] shown in panel (a).

synthetic cross sections are characterized by the occasional structure with a width several times the coherence width of the underlying compound-nucleus states. James and Fletcher have observed similarly broad structures in their data about which they have noted that there is "some evidence for overlapping structures" [7].

Figure 6 shows the rapid changes in the shapes of the synthetic angular distributions that accompany the fluctuations in the total $^8Be_0$ cross-section excitation function of Fig. 5(b). The fluctuations in the differential cross sections are correlated over a large angular range. For

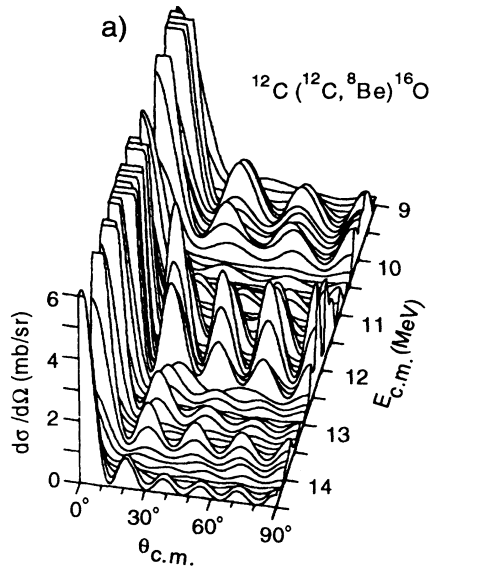

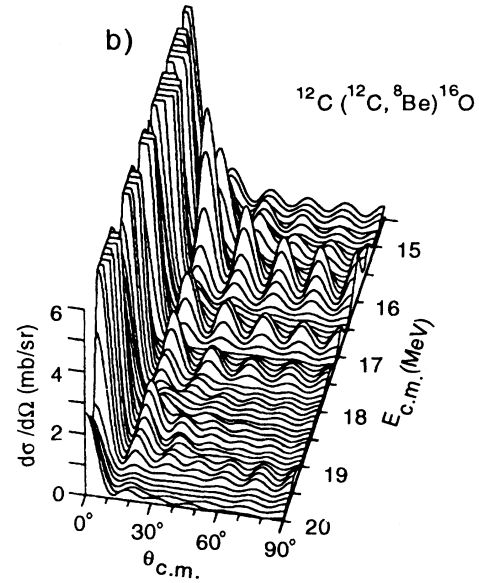

FIG. 6. Synthetic angular distributions calculated for the $^{12}C(^{12}C,^8Be_0)^{16}O$ reaction. These angular distributions were synthesized by the same calculation that generated the excitation function of total cross sections shown in Fig. 5(b). The cross sections saturate at 6 mb/sr.

a spin-zero exit channel such as $^8Be_0$, angular distributions that are dominated by a particular J value exhibit a characteristic $P_L^2(\cos\theta)$ shape with $L = J$. The shapes of the angular distributions near fluctuation maxima in the total cross section indicate that the majority of the peaks within a range of energies spanning several MeV are dominated by a single spin value. A given spin usually dominates peaks in the energy region where its HF partial cross exceeds all other partial cross sections [see Fig. 4(a)], i.e., $J = 6$ at energies $\lesssim 11$ MeV, $J = 8$ for $E_{c.m.} \approx$ 11–14 MeV, $J = 10$ for $E_{c.m.} \approx 14$–18 MeV, and $J = 12$ at higher energies. Within each of the gross structure regions, individual fluctuations can exhibit peak-to-valley ratios for the resonating partial cross section exceeding 10:1, a value much larger than maximum ratio in the total cross section. A good example of the abrupt variations of the individual partial cross sections is seen in Fig. 6(a) where $J = 8$ dominates the angular distributions at 12.6 and at 12.8 MeV, but the angular distribution in between exhibits a shape characteristic of a larger $J = 6$ contribution. The number of overlapping compound-nucleus levels that contribute to the resonating partial wave varies considerably over its region of dominance. Values of $\Gamma^J/D^J \approx 4$ and $\Gamma^J/D^J \approx 20$, respectively, constitute the rough lower and upper bounds for the degree of overlap where a fluctuation dominated by spin J is likely to occur in this reaction channel.

The gross structure regions of $J = 8$, 10, and 12 dominance in the synthetic cross sections approximate the energy ranges where Fletcher *et al.* [4] have observed similar enhancements in angular distributions measured at angles from $\theta_{c.m.} \approx 12°$ to 66°. The $J = 6$ strength at the lowest energies is more easily identified in Fig. 6(a) than in the angular distributions shown in Ref. [4], although later measurements, which extend the covered angular range, reveal several predominantly $J = 6$ peaks in this region [7].

A set of excitation functions of total cross sections synthesized at 50-keV intervals from $E_{c.m.} = 6.5$ to 12.6 MeV for the $^{12}C(^{12}C,\alpha)^{20}Ne^*$ reactions leading to the first six residual states is shown in Fig. 7. Since the compound states populated by the $^{12}C+^{12}C$ interactions are the same for each of these reactions, the same set of compound-nucleus level energies and entrance channel amplitudes is used for all of the reactions. A different set of exit channel amplitudes is employed for each of the reaction channels as described in Sec. II. The agreement between the data, shown in Fig. 2, and the simulations as to the magnitude of the cross sections and density of maxima for these α-particle channels approaches that obtained at mostly higher energies for the $^8Be_0$ channel. The comparisons of principal interest are those involving the excitation functions for cross sections summed over several exit channels. Fluctuations appear in the summed excitation functions for both the data and the synthesized cross sections. Structure survives whether the cross sections are summed over the 6, or 12, lowest excitations of ^{20}Ne. The uppermost synthetic excitation function in Fig. 7 shows the effect of increasing the number of channels in the sum to 21. Little effect is seen at the lowest reaction energies where the cross sections for the higher excitations are small. Because of the increased contributions from the additional channels, dampening of the structure from the final states with the lowest excitations is apparent at higher reaction energies, but fluctuations persist.

Some differences in detail are found between the data and the simulations. The average magnitude of the synthetic cross sections summed over the states α_0 to α_{11} is smaller than their counterparts in the data. This difference reflects the contributions of direct reactions to the experimental cross sections as discussed in Sec. III. The structure in the summed excitation functions for the data is slightly narrower than in that in the simulations, and more small peaks survive in the data. This result suggest that the average coherence width of the underlying compound states in this energy region is somewhat smaller than that obtained from the parametrization expressed by Eq. (6). While considering the importance of the differences in the number of surviving small peaks, it is appropriate to point out that some of the peaks in the published data of Voit *et al.* [6] are defined by a

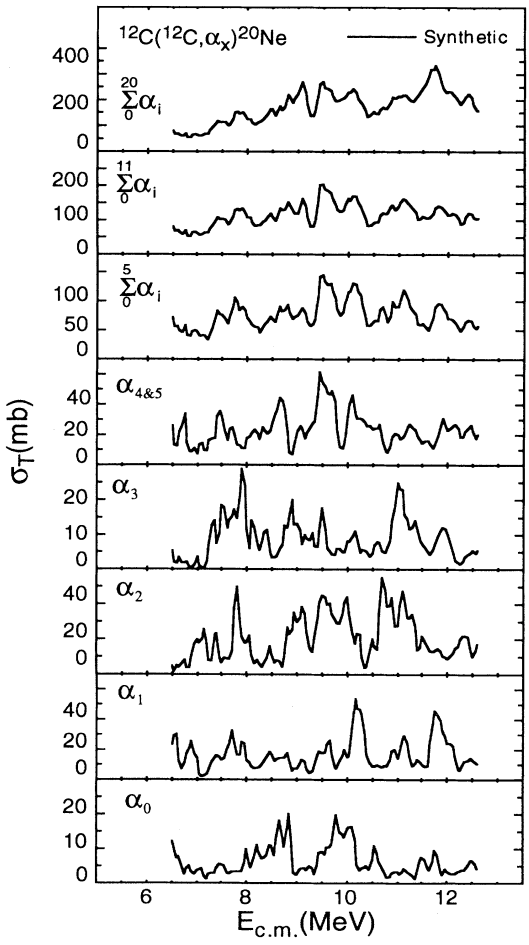

FIG. 7. Synthetic excitation functions of total cross sections calculated for the $^{12}C(^{12}C,\alpha)^{20}Ne^*$ reactions leading to the first six states in ^{20}Ne. The excitation functions shown in the three uppermost panels include total cross sections summed over the first 6, 12, and 21 states in ^{20}Ne.

single data point in the summed cross section and might be a consequence of the relative statistical errors in the cross sections. The authors in Ref. [6] report dominant J^π values for maxima which appear in either of the two lowest 0^+ α-particle channels and which persist in the summed cross sections. They report "resonances" that are grouped according to spin with $J = 4$, 6, and 8 dominating in succession as the reaction energy increases. The simulations also show peaks that result from a single resonating partial cross section, but maxima dominated by $J = 2$, 4, or 6 are interspersed throughout the energy region below $\approx$9.5 MeV, and the region between $\approx$9.5 and $\approx$12.6 MeV includes both $J = 6$ and 8 dominated peaks. Simulations which extend the α_0 cross sections up to 20 MeV show gross structure regions similar to those discussed above for the $^8Be_0$ channel.

V. SYSTEMATICS OF RESONANT FLUCTUATIONS

Figure 8 summarizes the results of this study of the resonant characteristics of fluctuations. At this juncture, it is convenient to let the phrase "resonant fluctuation" designate a fluctuation that is dominated by a single, resonating partial cross section. In Fig. 8, a rectangle encloses a range of energies for each of the even spin values from $J = 2$ to 12. The minimum energy enclosed for each spin coincides with the lower limit of the statistical region, that is, where $\Gamma^J/D^J = 2$. The top of each rectangle is at the energy where $\Gamma^J/D^J = 20$, which is roughly the maximum degree of overlap for which a resonant fluctuation dominated by spin J is likely to be observed. It is possible that a resonant fluctuation of spin J that appears near the lower boundary of its statistical region is dominated by the character of an individual compound-nucleus level. At the other extreme, the number of interfering levels is an order of magnitude larger near the upper limit and the probability that a resonant fluctuation is dominated by an individual level is reduced accordingly. The trajectory of the $^{12}C+^{12}C$ grazing angular momentum intersects the rectangles for $J = 2$, 4, 6, and 12 at energies well above the lower limit of the statistical region, but approaches the lower limit for $J = 8$ and 10. Thus compound-nucleus levels with degrees of overlap that can lead to resonant fluctuations are populated over a broader range of energies for $J = 8$ and 10 than for the lower J values. The gross structure regions in which $J = 8$, 10, and 12 in succession dominate the resonant fluctuations occur at energies above the grazing angular momentum trajectory. For each of these J values, the gross structure region appears above the upper limit of resonant fluctuations for $J - 2$ and below the grazing energy for $J + 2$. These conditions do not occur for the lower spins. The absence of predominantly $J^\pi = 0^+$ resonant structure above the barrier region is considered within the framework of resonant fluctuations to be a consequence of the $2J + 1$ dependence of the entrance channel flux. The grazing energy for $J = 0$ is not much lower than those for $J = 2$ and 4, but the flux populating compound states with $J = 2$ or 4 is overwhelmingly larger than that for $J = 0$.

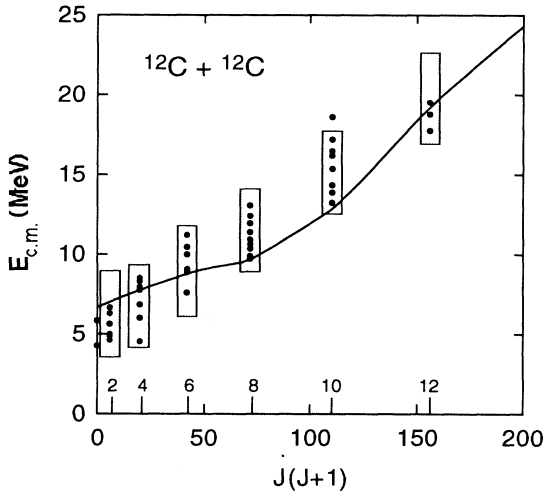

FIG. 8. Reaction energy versus angular momentum for resonant fluctuations and "resonances" in $^{12}C+^{12}C$ reactions. The rectangular box for each J value indicates the energy region where fluctuations in total cross sections for $^8Be_0$ and α-particle exit channels are likely to be dominated by a single resonant partial cross section with spin J. The solid circles indicate the energies and spins of "resonances" taken from summaries in Refs. [7] and [10] and include structures seen in other exit channels in addition to those observed in $^8Be_0$ and α-particle exit channels. The solid line indicates the grazing energy for each spin at which the transmission coefficient calculated for the $^{12}C+^{12}C$ entrance channel has a value $T_c^J = 0.5$.

A summary of reported $^{12}C+^{12}C$ "resonances" is displayed in Fig. 8. The displayed energies and spins of the resonances are taken from summaries in Refs. [7] and [10]. The summary shows "resonances" in the near-barrier region along with those above the barrier in the region of the simulations discussed above. The displayed "resonances" include structures observed in several $^{12}C+^{12}C$ exit channels in addition to those seen in the ^8Be and α-particle channels. The comparison above the barrier region shows that "resonances" and resonant fluctuations with the same spin are likely to occur within the same range of energies. While this result does not impute a statistical origin for any particular "resonance," previously drawn conclusions concerning the nature of many of these "resonances" are based on the observation of properties in the data that have been demonstrated here as also characterizing fluctuations. The list of experimental and analytical techniques available for discerning nonstatistical "resonances" from Ericson fluctuations in the data for, at the very least, the reaction channels examined in the present work is restricted. Since criteria that require the appearance of structure in angle-integrated cross sections, correlation with a dominant resonating partial wave, and/or the appearance of structure in cross sections summed over many exit channels are not sufficient, the utility of other methods should be examined. The principal techniques that remain viable involve tests that search data for nonstatistical correlations between structures in different exit channels, such

as those that appear in $^{12}C+^{12}C$ reaction channels below the Coulomb barrier or where many exit channels are open, structures with unusually large branching ratios to several intrinsically related exit channels, such as to residual states that are members of a rotational band. The effectiveness of several types of statistical tests in locating "resonances" were examined in an earlier publication [44].

Several future projects are suggested by this work. Perhaps the most critical is an extensive study of the correlations between resonant fluctuations in different exit channels. Although a limited study has been carried out and shown to predict small correlations, the results of the study may be sensitive to the number of low spins included explicitly in the sums over compound-nucleus levels used to calculate the collision matrix. The study of correlations between different exit channels needs to be repeated using more low spin levels. Fluctuation simulations should be extended to other exit channels. In particular, synthetic excitation functions and angular distributions calculated for the elastic channel will provide information on the size and frequency of fluctuations in the total $^{12}C+^{12}C$ reaction cross section. The accurate simulation of elastic cross sections requires an optical-model calculation at each energy. Finally, simulations should be carried out for other systems of interacting nuclei where "resonances" have been reported. Simulations of interactions involving nonidentical nuclei, such as $^{12}C+^{16}O$, can be used to examine the effects on the shapes of angular distributions of contributions from compound-nucleus levels with odd, as well as even, spin values. Completing these projects will require extensive revision of the current simulation code, and many hours of computer time will be accumulated before quantitative estimates of cross-channel correlations can be made.

VI. SUMMARY

Comparisons of Hauser-Feshbach calculations to measured total cross sections for ^{8}Be and α-particle exit channels of the $^{12}C+^{12}C$ system indicate that the majority of these reactions are compound nucleus in nature. The Hauser-Feshbach calculations show that, on the average, significant contributions to the cross sections are limited to a narrow range of spin values. The statistical-model simulations of angular distributions and excitation functions performed in this work produce results that are in overall quantitative agreement with the size and frequency of fluctuations observed in measured total cross sections. Because of the restrictions imposed by the conservation of angular momentum, many of the synthetic fluctuations are dominated by a single resonating partial cross section. The simulations systematically reproduce the spins that dominate the structures observed in the data. Without explicitly including isolated "resonances" in the model, virtually all of the resonance effects found at energies above the Coulomb barrier in these $^{12}C+^{12}C$ reaction channels have been explained.

ACKNOWLEDGMENTS

This work was supported in part by the National Science Foundation under Grant No. PHY-8900689 (FSU) and by a University of North Florida Academic Affairs/College of Arts and Sciences Summer Research Award. Figures for this paper were constructed with the aid of L. Burns, K. Ford, and W. Thorner. It is a pleasure to thank S. M. Grimes of Ohio University for supplying pertinent information on nuclear level densities and N. R. Fletcher for a critical reading and discussion of this work.

[1] E. Almqvist, D. A. Bromley, J. A. Kuehner, and B. Whalen, Phys. Rev. Lett. **4**, 515 (1960).
[2] T. Ericson, Phys. Rev. Lett. **5**, 430 (1960).
[3] J. A. Kuehner, J. D. Prentice, and E. Almqvist, Phys. Lett. **4**, 332 (1963).
[4] N. R. Fletcher, J. D. Fox, G. J. KeKelis, G. R. Morgan, and G. A. Norton, Phys. Rev. C **13**, 1173 (1976).
[5] K. A. Erb, R. R. Betts, D. L. Hanson, M. W. Sachs, R. L. White, P. P. Tung, and D. A. Bromley, Phys. Rev. Lett. **11**, 670 (1976).
[6] H. Voit, W. Galster, W. Treu, H. Fröhlich, and P. Dück, Phys. Lett. **67B**, 399 (1977).
[7] D. R. James and N. R. Fletcher, Phys. Rev. C **20**, 560 (1978).
[8] N. Cindro, F. Coçu, J. Uzureau, Z. Bazrak, M. Cates, J. M. Fieni, E. Holub, Y. Patin, and S. Plattard, Phys. Rev. Lett. **39**, 1135 (1977).
[9] A. Kapuścik, R. Zybert, M. Pajek, J. Ploskonka, and L. Zybert, Nucl. Phys. **A383**, 530 (1982).
[10] K. A. Erb and D. A. Bromley, Phys. Rev. C **23**, 2781 (1981).
[11] E. Almqvist, J. A. Keuhner, D. McPherson, and E. W. Vogt, Phys. Rev. **136**, B84 (1964).
[12] D. Shapira, R. G. Stokstad, and D. A. Bromley, Phys. Rev. C **10**, 1063 (1974).
[13] T. Ericson, Ann. Phy. (N.Y.) **23**, 390 (1963).
[14] P. J. Dallimore and I. Hall, Nucl. Phys. **88**, 193 (1966).
[15] A. Van der Woude, Nucl. Phys. **80**, 14 (1966).
[16] P. G. Bizzeti and P. R. Maurenzig, Nuovo Cimento B **17**, 173 (1967).
[17] L. C. Dennis, Phys. Rev. C **27**, 2641 (1983).
[18] W. Hauser and H. Feshbach, Phys. Rev. **87**, 366 (1952).
[19] D. L. Gay, N. R. Fletcher, and L. C. Dennis, Phys. Rev. C **58**, 1512 (1987).
[20] J. M. Blatt and L. C. Biedenharn, Rev. Mod. Phys. **24**, 258 (1952).
[21] L. C. Biedenharn, J. M. Blatt, and M. E. Rose, Rev. Mod. Phys. **24**, 249 (1952).
[22] D. L. Gay, Ph.D. dissertation, Florida State University 1986.
[23] A. Gilbert and A. G. W. Cameron, Can. J. Phys. **43**, 1446 (1965).

[24] T. E. Ericson, Phys. Lett. **4**, 258 (1963).
[25] T. E. Ericson and T. Mayer-Kuckuk, Annu. Rev. Nucl. Sci. **16**, 183 (1966).
[26] D. M. Brink and R. O. Stephen, Phys. Lett. **5**, 77 (1963).
[27] R. G. Stokstad, in *Proceedings of the International Conference on Reactions Between Complex Nuclei* Nashville, Tennessee, 1974, Vol. 2, edited by R. L. Robinson, F. K. McGowan, J. B. Hall, and J. H. Hamilton (North-Holland, Amsterdam, 1974), Vol. 2, p. 327.
[28] L. Schrage, ACM Trans. Math. Software **5**, 132 (1979).
[29] E. W. Vogt, D. McPherson, J. Kuehner, and E. Almqvist, Phys. Rev. **136**, B99 (1964).
[30] H. V. Klapdor, G. Rosner, H. Reiss, and M. Schrader, Nucl. Phys. **A244**, 157 (1975).
[31] H. V. Klapdor, H. Reiss, and G. Rosner, Nucl. Phys. **A262**, 157(1976).
[32] L. C. Dennis, A. Roy, A. D. Frawley, and K. W. Kemper, Nucl. Phys. **A359**, 359 (1981).
[33] U. Faccini and E. Saetta-Menichella, Energ. Nucl. (Milan) **15**, 54 (1968).
[34] S. K. Penny, computer code HELGA (unpublished).
[35] M. Beckerman, Nucl. Phys. **A278**, 333 (1977).
[36] S. M. Grimes, Ohio University (private communication).
[37] K. Bethge, C. M. Fou, and R. W. Zurmühle, Nucl. Phys. **A123**, 521 (1969).
[38] K. Hatogai, M. Ohta, and S. Okai, Prog. Theor. Phys. **68**, 2014 (1982).
[39] D. G. Kovar, D. F. Geesamen, T. H. Braid, Y. Eisen, W. Henning, T. R. Ophel, M. Paul, K. E. Rehm, S. J. Sanders, P. Sperr, J. P. Schiffer, S. L. Tabor, S. Vigdor, and B. Zeidman, Phys. Rev. C **20**, 1305 (1979).
[40] J. W. Frickey, K. A. Eberhard, and R. H. Davis, Phys. Rev. C **4**, 434 (1971).
[41] R. Middleton, J. D. Garrett, and H. T. Fortune, Phys. Rev. Lett. **27**, 950 (1971).
[42] L. R. Greenwood, R. E. Segel, K. Raghunathan, M. A. Lee, H. T. Fortune, and J. R. Erskine, Phys. Rev. C **12**, 156 (1975).
[43] B. Strohmaier, S. M. Grimes, and H. Satyanarayana, Phys. Rev. C **36**, 1604 (1987).
[44] L. C. Dennis, S. T. Thornton, and K. R. Cordell, Phys. Rev. C **19**, 777 (1979).